Carbon/Carbon Composites Derived from Poly(ethylene oxide)-Modified Novolac-Type Phenolic Resin: Microstructure and Physical, and Morphological Properties

ALBERT Y. C. HUNG,[1] FENG-YIH WANG,[2] SHANG-RU YEH,[2] WEI-JEN CHEN,[2] CHEN-CHI M. MA[2]

[1] Department of Food Nutrition, Chung Hwa College of Medical Technology, No. 89, Wen-Hwa First St. Jen-Te Hsiang, Tainan Hsien, Taiwan, 71741, Republic of China

[2] Department of Chemical Engineering, National Tsing-Hua University, Hsin-Chu, Taiwan, 30043, Republic of China

Received 29 October 2000; accepted 10 January 2001

ABSTRACT: A poly(ethylene oxide) (PEO) novolac-type phenolic resin blend was prepared by the physical blending method. The modified novolac-type phenolic resin with various PEO contents was used as a matrix precursor to fabricate carbon/carbon composites. The effect of the PEO/phenolic resin mixing ratio on the change of the density and of the porosity was studied. The flexural strength and interlaminar shear strength of the PEO/phenolic resin blend-derived carbon/carbon composites were also investigated. The results show that the density of the PEO/phenolic resin blend-derived carbon/carbon composites decreases with the PEO content. The X-ray diffraction and Raman spectra studies showed that the carbon fiber in the samples will affect the growth of the ordered carbon structure. From SEM morphological observation, it is shown that the fracture surface of specimens is smooth. Also, there is less fiber pull-out and fiber breakage on the fracture surface. © 2002 Wiley Periodicals, Inc. J Appl Polym Sci 84: 1609–1619, 2002; DOI 10.1002/app.10407

Key words: carbon/carbon composite; X-ray diffraction; Raman spectra; mechanical properties

INTRODUCTION

Carbon fiber-reinforced carbon matrix (C/C) composites are unique materials that possess excellent properties such as high specific strength, high thermal stability, and low density. Furthermore, their ability to retain mechanical properties, at temperatures as high as 2000°C, is the most attractive characteristic of C/C composites. Hence, C/C composites have been utilized for rocket nozzles, disc brakes, and thermal insulating components.[1,2]

Phenolic resin has widely used in industry because of its good flame retardance, electrical insulation, dimensional stability, and chemical resistance.[3–6] However, the poor wet-out between carbon fiber and phenolic resin and the brittleness of phenolic resin are serious problems of the carbon fiber-reinforced phenolic composite. All the mechanical properties of modified phenolic resin can be increased by adding a thermoplastic modifier. For example, either ester groups or other hydrogen-bonding functional groups are more flexible than is phenolic resin. Hence, modified phenolic resin, which will absorb more loads, can improve the brittleness of novolac-type phenolic resin.[7,8]

Correspondence to: A. Y. C. Hung.

Journal of Applied Polymer Science, Vol. 84, 1609–1619 (2002)

Table I Materials Used in This Study

Materials	Description	Suppliers
Phenolic resin	GWL-3580 novolac-type	Quen Mo Chemical Co. (Taipei, Taiwan)
Carbon fiber	PAN base, #3085 plain woven	Mitsubishi Rayon Co. (Tokyo, Japan)
PEO	$(—CH_2CH_2O—)_n$	Aldrich Chemical Co. (Milwaukee, WI)
Hexamine	$C_6H_{12}N_4$	Acros Organics (Morris Plains, NJ)
Ethanol	95.0%	Shimakyu Chemical Co. (Osaka, Japan)

In this study, the physical and mechanical properties such as density, porosity, flexural strength, and flexural modulus of the C/C composites were investigated. The effect of carbon fiber on the microstructure of carbonized products was examined by X-ray diffraction (XRD) and Raman spectra. The morphology of the fracture surface of specimens was examined by SEM.

EXPERIMENTAL

Materials

The materials used in this study are listed in Table I. Hexamethylene tetramine (hexamine) was used as a curing agent and ethanol was used as a solvent. The content of the curing agent and solvent in all the samples were constant. The carbon fiber (PAN base, #3085, plain woven) used had a woven thickness of 1.6 mm and was supplied by the Mitsubishi Rayon Co., Ltd. (Japan).

Sample Preparation

Compositions of the tested samples are summarized in Table II. The poly(ethylene oxide) (PEO) novolac-type phenolic resin blend was prepared by the physical blending method.[7,8] The carbon fiber mat was cut into 200 × 200 × 1.6-mm^3 (length × width × thickness) pieces and then wet-out with modified phenolic resin. The processing procedures of carbon fiber-reinforced PEO/novolac-type phenolic blends-based composites were as follows:

(a) Preparing the carbon/carbon composite precursor (postcured product with carbon fiber, *postcured composites*):

The dimensions of the compression mold were 200 × 200 × 15-mm^3 (length × width × thickness). The heating temperature profile of the mold used two heating plates along the compression direction. The surfaces of the stainless-steel mold were treated with chromium plating. The carbon fiber prepared with modified phenolic resin was put in an oven at 80°C for 6 h and then transferred to a hot press (170°C, 1000 psi) for 30 min. The postcuring temperature was 180°C for 24 h to ensure complete reaction of the modified phenolic blend. Simultaneously, the residual solvent and water in the specimens were removed completely.

(b) Precursor to prepare carbonized carbon/carbon composite (carbonized product with carbon fiber; *C/C composites*):

The fabricated PEO-modified phenolic resin/carbon fiber composites were cut into 50.0 × 10.0

Table II Compositions of Tested Samples

PEO Content (phr)	Phenolic (g)	PEO (g)	Hexamine (g)
0	50	0	5.0
5	50	2.5	5.0
10	50	5.0	5.0
15	50	7.5	5.0

Carbon fiber content of the tested samples: 68 wt %.

$\times$ 1.5-mm^3 specimens and then were carbonized at 1050°C under a nitrogen atmosphere for 60 min to form the C/C composites.

(c) Carbonized novolac-type phenolic resin with various PEO contents (carbonized product without carbon fiber, *carbonized composites*):

The mold size was 50.0 $\times$ 10.0 $\times$ 1.5-mm^3. The modified phenolic resin was put in an oven at 80°C for 6 h and then the temperature was increased to 170°C overnight in a vacuum. The postcuring temperature was 180°C for 24 h to ensure complete reaction of the modified phenolic blend. Certainly, the residual solvent and water in the specimens were also removed during the treatment. The postcured samples were carbonized at 1050°C under a nitrogen atmosphere for 60 min.

Properties and Morphology Investigations

Density and Porosity

The densities of the C/C composites were measured on a Precica 180A microbalance using the water-immersion method. According to the ASTM C-20 method, the open porosity was measured by boiling water penetration. The specimens were immersed in boiling water for 2 h. Air in the pores was assumed to be replaced by water during the boiling process. After the specimen was cooled to room temperature, water on the specimen surface was removed carefully and the weight of the specimen filled with water was measured. The percentage of open porosity was determined by the following equation[9]:

$$\text{Open porosity } (\%) = \frac{W_w - W_d}{W_d/D} \times 100\%$$

where W_w is the weight of the specimen after being immersed in boiling water for 2 h; W_d, the weight of the dried specimen; and D, the density of the specimen.

Flexural Properties

Three-point bending tests with a span-to-depth ratio of 30 mm and a crosshead speed of 1.0 mm/min were performed in an Instron test machine (Model 4468). The flexural strength of the C/C composites was measured by the ASTM D-790 method.

Interlaminar Shear Strength (ILSS)

ILSS tests, with a span-to-depth ratio of 4 mm and a crosshead speed of 1.3 mm/min, were performed in an Instron test machine (Model 4468). The ILSS of the C/C composites was measured according to the ASTM D-2344 method.

Microstructure

A Rigaku B/MAX-11B X-ray analyzer was utilized to measure the d_{002} basal plane interlayer spacing. All specimens were analyzed by copper radiation using a computer-controlled powder diffractometer at a speed of 4°/min under 30 kV and 20 mA. The Raman spectrometer used was a Reinshaw, Raman imaging microscope system 2000. The calculation is based upon Bragg's Law[10]:

$$n\lambda = 2d \sin \theta \tag{1}$$

The average crystallite dimension in the c-direction (stacking height of crystallite, Lc) was calculated according to the Scherrer equation[11]:

$$L_c = \frac{0.9\lambda}{(\Delta 2\theta)\cos \theta} \tag{2}$$

where λ is the wavelength of the X-ray radiation; d, the basal plane interlayer spacing; θ, the Bragg angle; n, an integer; and $\Delta 2\theta$, the half-height width of the diffraction intensity distribution (measured in radians). The monochromatic light source was an Ar^+ laser (514.5 nm). The morphological observations of the fracture surface of the C/C composites were examined by a scanning electron microscope (JEOL JSM 840A, JEOL Co., Japan).

RESULTS AND DISCUSSION

Density

Figure 1 shows a comparison of the densities of the postcured composites and the C/C composites. The density of the C/C composites is lower than that of the postcured composites, due to the modified phenolic resin degrading completely from the carbonizing process.

Porosity

Figure 2 shows a comparison of the porosity of the postcured composites and the C/C composites. The porosity of postcured composites was kept constant, even though the PEO contents were changed. That of the C/C composites increased

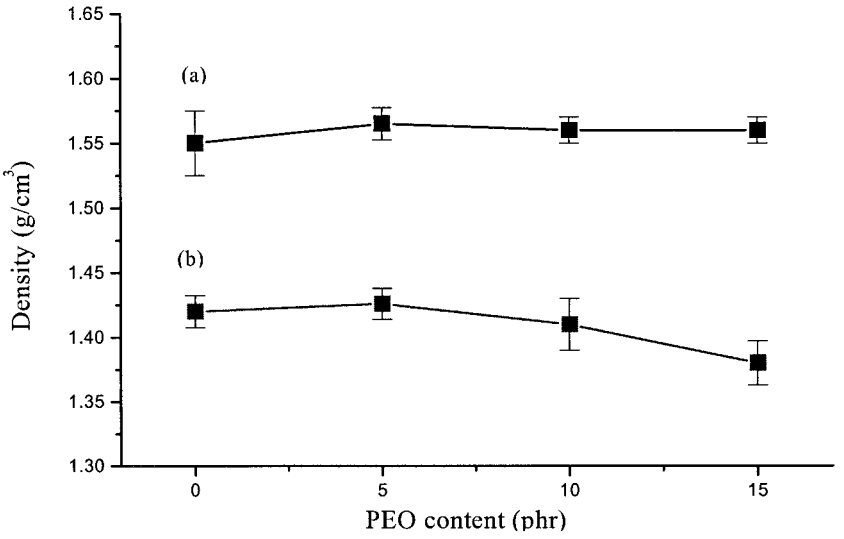

Figure 1 Density of (a) postcured composite and (b) C/C composite of 2D carbon fiber-reinforced phenolic resin with various PEO contents.

with various PEO contents. The modified phenolic resin degraded to generate gas molecules such as CH_4, H_2, CO_2, and CO.[12] Due to the modified phenolic resin degradation, the change of the porosity should be consistent with the change of density. Pure PEO degrades completely at 400°C and the degradation temperature of phenolic resin is higher than that of PEO.[12] Comparing the results of Figures 1 and 2, the porosity increased with the PEO contents in the C/C composites. Consequently, the density decreased with increased PEO contents in the C/C composites.

Flexural Properties and Interlamilar Shear Properties

Figure 3(a) shows the flexural strength of the postcured composites. There is an optimal flexural strength of the postcured composites with 5 phr PEO, because PEO can react with phenolic resin to form stronger intermolecular hydrogen bonding and PEO is a high crystalline thermoplastic polymer. Since the crystallinity potential of PEO is higher than is the intermolecular hydrogen bonding, the wet-out of modified phenolic

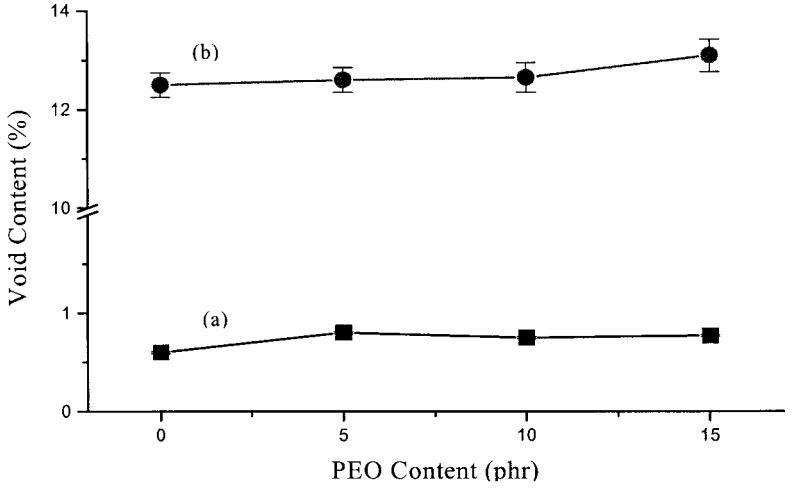

Figure 2 Porosity of (a) postcured composite and (b) C/C composite of 2D carbon fiber-reinforced phenolic resin with various PEO contents.

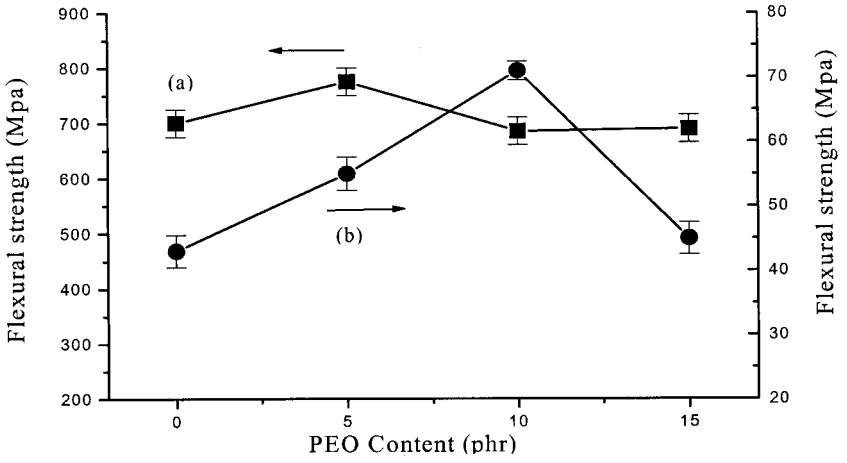

Figure 3 Flexural strength of (a) postcured composite and (b) C/C composite of 2D carbon fiber-reinforced phenolic resin with various PEO contents.

resin with higher PEO content is poor.[8] In other words, the wet-out affects the mechanical properties of postcured composites.[8] Figure 3(b) shows the flexural strength of the C/C composites. The flexural strength of the modified phenolic resin is higher than that of the pure phenolic resin. The effects on the flexural strength of the C/C composite by the carbonization process are due to internal stress and composite volume shrinkage. The degradation temperature of PEO was about 400°C. In the degradation process, the phenolic resin degraded partially but the PEO degraded completely.[11] The PEO degrades completely to form channels in the C/C composite so that the formed gas is able to flow out by degradation. This is the reason why the internal stress is decreased. However, when the PEO content is too high, then it forms too many voids in the C/C composite that can cause microcracks and the flexural strength decreases.

Figure 4 indicates the ILSS of postcured composites and C/C composites. The ILSS of this system is affected by (a) the bonding force between the matrix and the fiber and (b) voids and cracks formed in the composite by thermal treatment. Modification of the phenolic resin can improve the bonding force between matrix and fiber and, therefore, increase the ILSS of postcured products. When 15 phr PEO is blended with phenolic resin, microcrystalline domains of PEO are formed, and, hence, the bonding force between the matrix and fiber is decreased.[8] As a result the

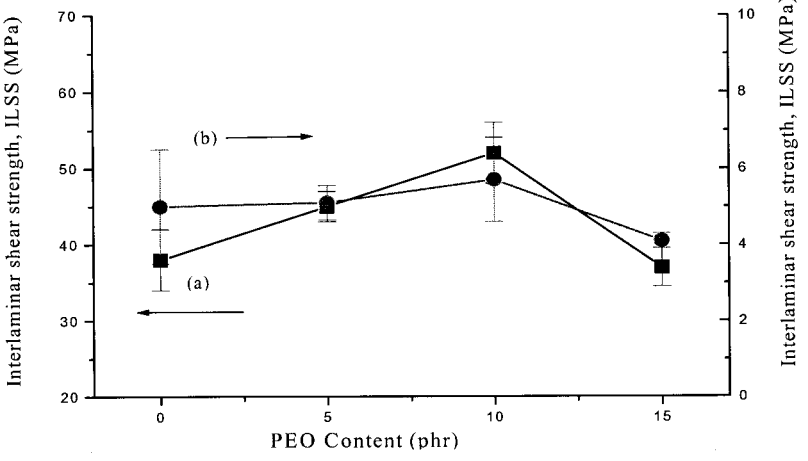

Figure 4 ILSS of (a) postcured composite and (b) C/C composite of 2D carbon fiber-reinforced pheolic resin with various PEO contents.

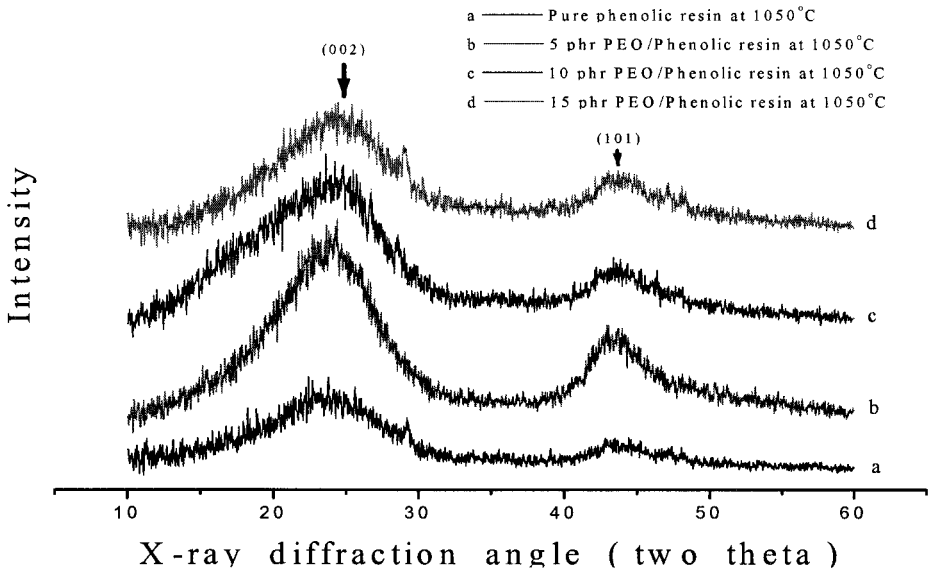

Figure 5 XRD curves of carbonized pure novolac-type phenolic resin with various PEO contents: (a) pure phenolic resin and (b) 5 phr PEO, (c) 10 phr PEO, and (d) 15 phr PEO/phenolic resin at 1050°C.

ILSS of postcured composites with 15 phr is lower than that of pure phenolic resin. The ILSS of C/C composites is not affected by the PEO content since the modified phenolic resin degraded completely. However, the modified phenolic resin improves the bonding between the matrix and the fiber before carbonization. After carbonization, the C/C composite volume is changed due to degradation of the modified phenolic resin. The ILSS of the C/C composite is slightly higher than that of the postcured composite.

Microstructures

Figure 5 shows the X-ray diffraction spectra of carbonized composites. The XRD spectra of C/C composites with various PEO contents are shown in Figure 6. In considering observations from both Figures 5 and 6, the former shows that PEO does not assist the growth of an ordered carbon structure or increase the amorphous carbon structure in the modified phenolic resin. According to Figure 6, the shape of the $d(002)$ peak is sharp and symmetric. Furthermore, the width of the $d(002)$ peak in Figure 6 is smaller than is the width of the $d(002)$ peak in Figure 5. It can be concluded that the carbon fiber assists the growth of ordered carbon structures.

Figure 7 shows the Raman spectra of carbonized composites. The Raman spectra of C/C composites with various PEO contents are shown in Figure 8. There are two specific absorption peaks for carbon materials located within the ranges of 1350–1380 cm^{-1} (D mode) and 1580–1600cm^{-1} (G mode), respectively. The D-mode peak results from short-range turbostratic structures (amorphous structure) and the G-mode peak represents the normal graphite structure.[13,14] The R value is the peak intensity ratio of the D mode to the G mode. The term "disordered" (in unit of percent) is calculated by dividing the D-mode intensity by the sum of the D-mode and the G-mode peak intensities. This illustrates the degree of the turbostratic structures inside the carbonized materials. Figure 9 shows the changes of the R value and the "disordered" for carbonized composites and C/C composite systems. It was found that the R value and the "disordered" of the C/C composites are smaller than are those of carbonized composites.

The structural parameters of the PEO-modified novolac-type phenolic resin-derived carbon materials can be determined from the XRD and Raman spectra. The calculation method of Lc from XRD was explained in the Experimental section. From the Raman spectra, the relationship between La (stacking length of crystallite) and the intensities of the D and G modes were derived from Tuinstra and Koeing[11]:

$$La = 44(I_D/I_G)^{-1} \quad (3)$$

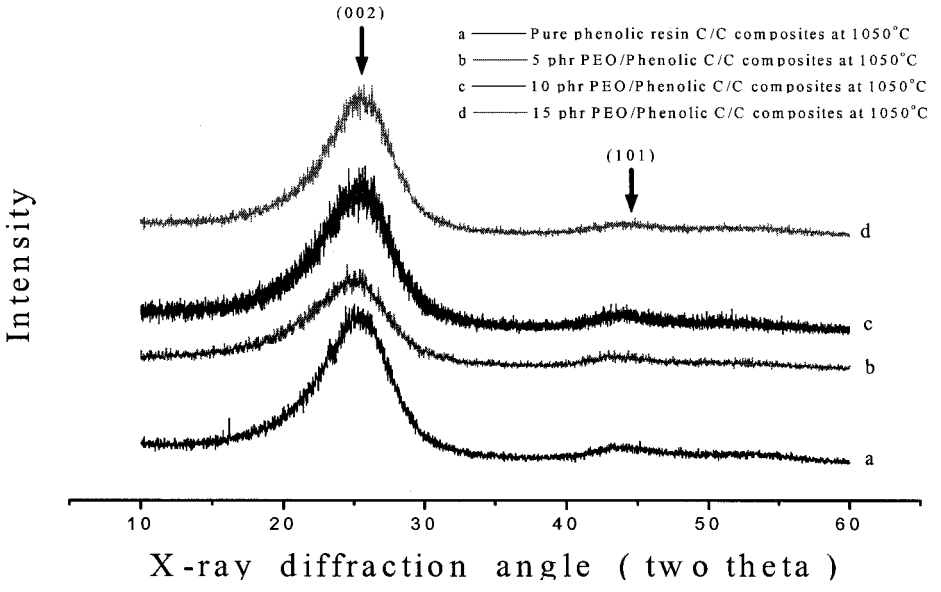

Figure 6 XRD curves of C/C composite with various PEO contents: (a) pure phenolic resin and (b) 5 phr PEO, (c) 10 phr PEO, and (d) 15 phr PEO/phenolic resin at 1050°C.

where I_D and I_G are the intensity of the D mode and the G mode in the Raman spectra, respectively. Figure 10 shows the calculated *Lc* and *La* values of the carbonized composites and C/C composites. It can be seen that the *Lc* and *La* values for the C/C composites are higher than are those of the carbonized composites. The "*Lc*/*d*002" (number of carbon interlayers) for various carbonized composites and C/C composites are shown in Figure 11, namely, *Lc*/*d*002 (number of carbon interlayers) was the ratio of the intensities of *Lc* and *d*002.[11,14] The results in Figure 11 are similar to those in Figure 10. This indicates that the growth of the crystallite height (*Lc*) and the crystallite length (*La*) was promoted by the carbon fiber. In general, the carbon fiber can affect the

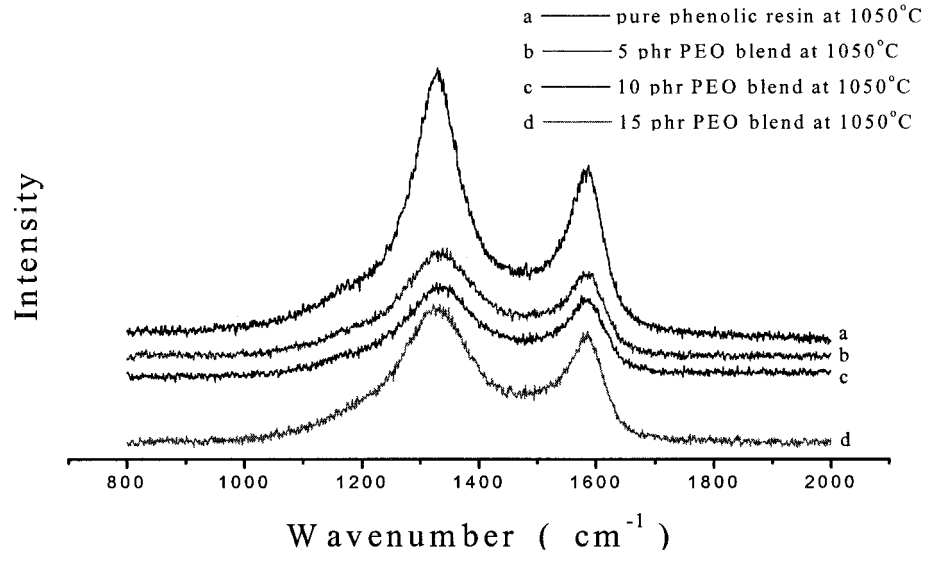

Figure 7 Raman spectra of carbonized novolac-type phenolic resin with various PEO contents: (a) pure phenolic resin and (b) 5 phr PEO, (c) 10 phr PEO, and (d) 15 phr PEO/phenolic resin at 1050°C.

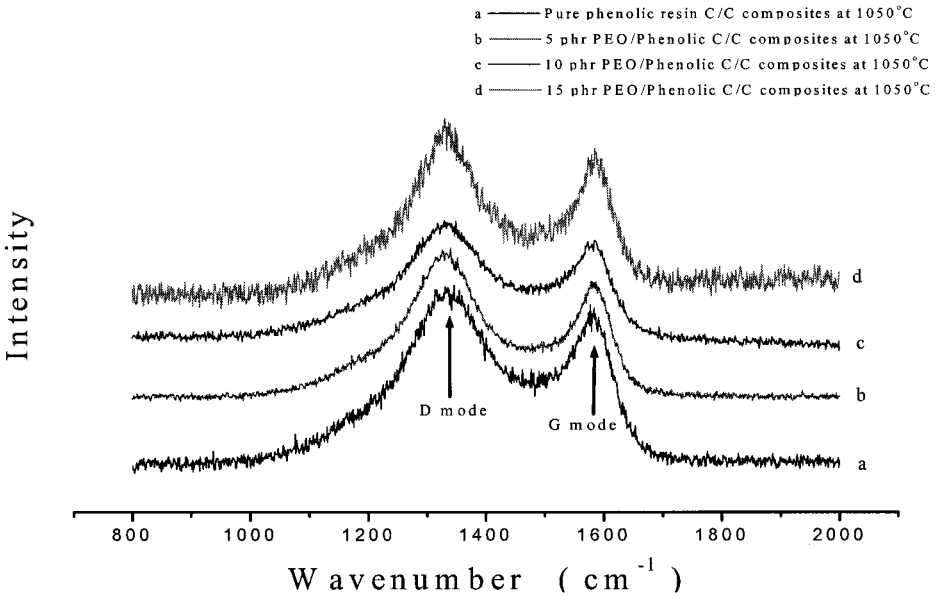

Figure 8 Raman spectra of C/C composite with various PEO contents: (a) pure phenolic resin, and (b) 5 phr PEO, (c) 10 phr PEO, and (d) 15 phr PEO/phenolic resin at 1050°C.

growth of the crystallite height (*Lc*) and crystallite length (*La*) of carbon materials.[11,14]

Morphological Properties

SEM investigations were applied to examine the morphology of the PEO-modified novolac-type phenolic resin-derived C/C composites. Figure 12(a)–(d) shows side-view SEM microphotographs of the fracture surface of C/C composites that are derived from phenolic resin and from 5, 10, and 15 phr PEO/phenolic resin. By comparing these figures, the fracture surface is smooth and slippery. There is less fiber pull-out and fiber breakage on

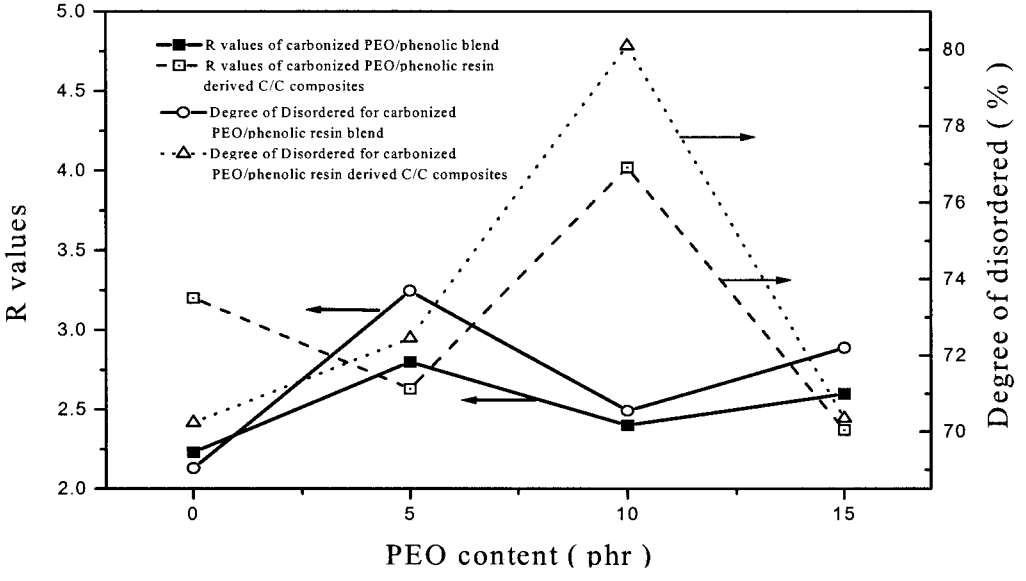

Figure 9 Degree of disordered carbon structure for various carbonized PEO/phenolic resin blends and C/C composites.

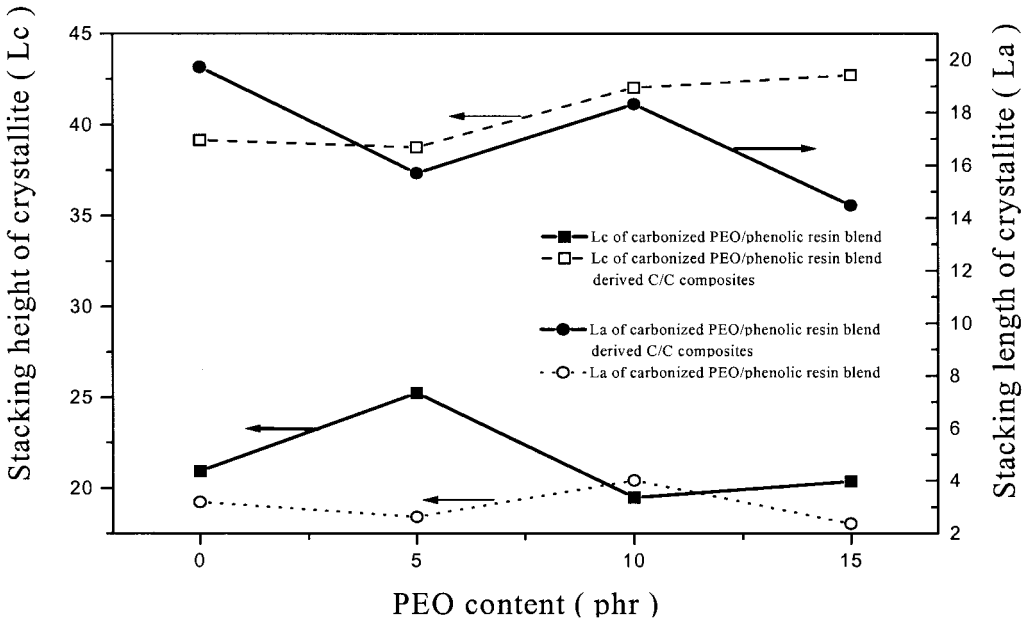

Figure 10 *Lc* (calculated from XRD) and *La* (calculated from Raman spectra) of carbonized PEO/phenolic resin blends and C/C composites.

the fracture surface. It is shown that the fracture type of the C/C composites, after carbonization is brittle fracture. However, there is no evidence to show a correlation between the PEO content and the fracture type of the C/C composites.

Figure 13(a)–(c) shows top-view SEM microphotographs of fracture surfaces of the C/C composites that are derived from phenolic resin and 10 and 15 phr PEO/phenolic resin. By comparing these figures, the surface bonding of the carbon

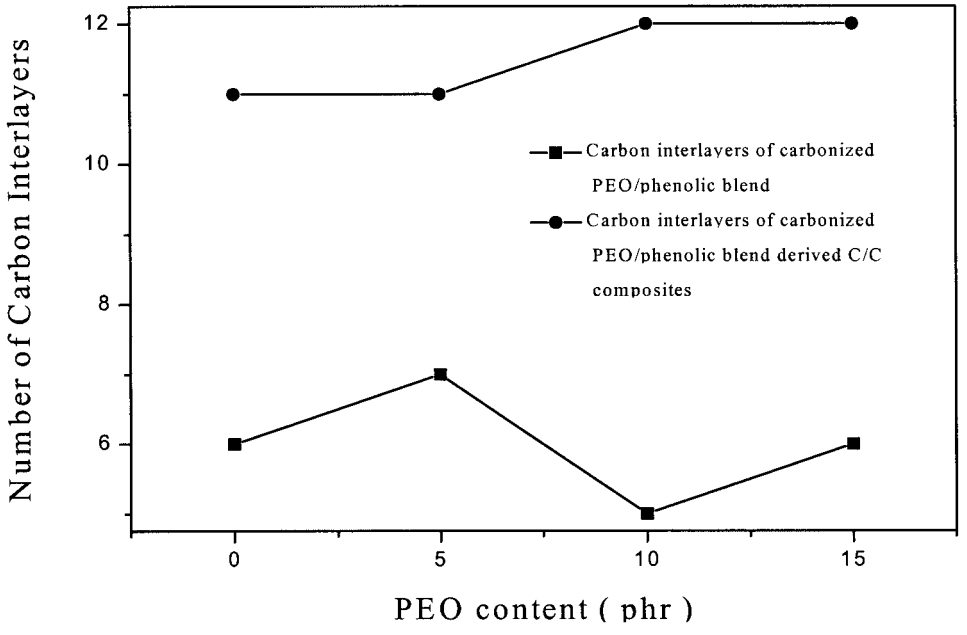

Figure 11 *Lc*/*d*002 (number of carbon interlayers[11,14]) for various carbonized PEO/phenolic resin blends and C/C composites.

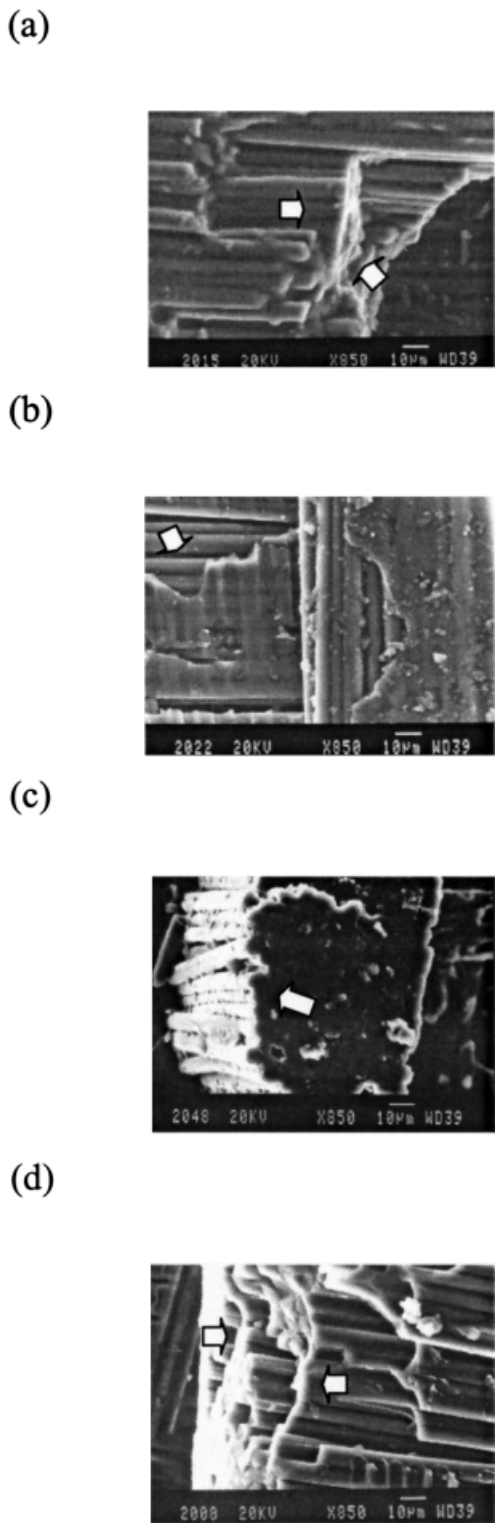

Figure 12 Side-view SEM micrograph of fracture surface of C/C composites derived from (a) phenolic resin and (b) 5 phr PEO, (c) 10 phr PEO, and (d) 15 phr PEO/phenolic resin.

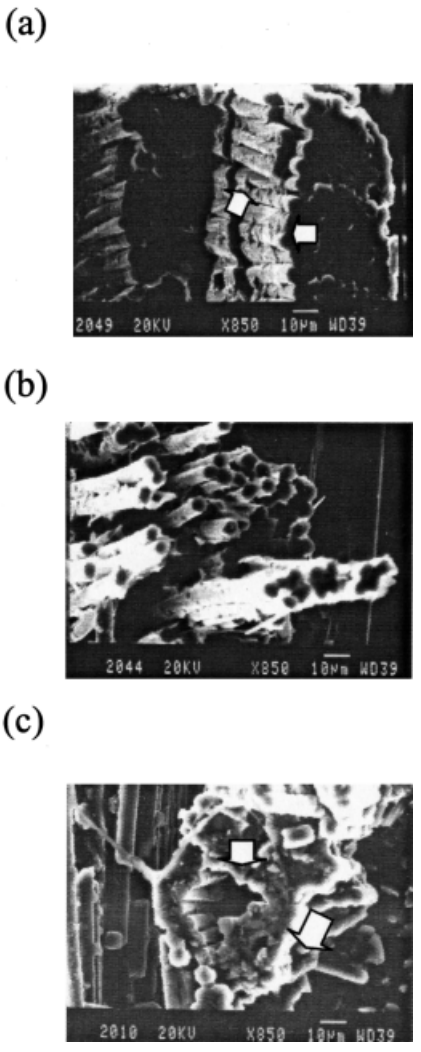

Figure 13 Top view SEM microphotograph of fracture surface of C/C composites derived from (a) phenolic resin, (b) 10 phr PEO/phenolic resin, (c) 15 phr PEO/phenolic resin.

matrix and carbon fiber, as shown in Figure 12(c), seems to be the best. However, the surface bonding of the carbon matrix and carbon fiber in the phenolic resin system is not as good as in the 10 phr PEO/phenolic resin system. In accordance with these observations, it can be concluded that the enhancement of the flexural strength and the ILSS of the PEO-modified novolac-type phenolic resin-derived C/C composites (as shown in Figs. 3 and 4) could bring about better interfacial bonding between the carbon fiber and the carbon matrix.

CONCLUSIONS

A PEO/novolac-type phenolic resin blend can be utilized to fabricate C/C composites. The effects of

the heat treatment, PEO content, and carbon fiber on the microstructure and physical and mechanical properties of C/C composites were also studied. The results show that the densities of the C/C composites are lower than are those of post-cured composites. There is an optimal flexural strength of the C/C composites with the 10 phr PEO-modified phenolic resin. The change of the ILSS of the C/C composites is similar to the tendency of the change of the flexural strength. The XRD and Raman spectra studies show that the growth of the stacking height of crystallites was promoted by the carbon fiber and the effect on the stacking length of the crystallites is significant. The improved interfacial bonding between the resin matrix and the carbon fiber will enhance the ILSS and flexural strength of a C/C composite.

REFERENCES

1. Chang, W. C.; Tai, N. H.; Ma, C. C. M. J Mater Sci 1995, 30, 1225.
2. Ma, C. C. M.; Tai, N. H.; Chang, W. C.; Tsai, Y. P. Carbon 1996, 34, 1175.
3. Wu, H. D.; Ma, C. C. M.; Lee, M. S.; Wu, Y. D. Angew Makromol Chem 1996, 235, 35–45.
4. Kershaw, D.; Still, R. H. J Appl Polym Sci 1975, 19, 973–981.
5. Wang, F. Y.; Ma, C. C. M.; Wu, H. D.; J Appl Polym Sci 1999, 74, 2283.
6. Lee, C. T.; Wu, H. D.; Chu, P.; Ma, C. C. M. J Polym Sci Part B Polym Phys 1998, 36, 1721.
7. Wang, F. Y.; Ma, C. C. M.; Wu, W. J. J Appl Polym Sci 1999, 73, 881–887.
8. Ma, C. C. M.; Lee, C. T.; Wu, H. D. J Appl Polym Sci 1998, 39, 703.
9. Annual Book of ASTM Standards; ASTM: Philadelphia, PA, 1991; C20–87.
10. Cullity, B. D. Elements of X-ray Diffraction, 2nd ed. Addison-Wesley: Reading, MA, 1978; pp 102.
11. Tuinstra, F.; Koeing, J. Q. J Chem Phys 1970, 53, 1126.
12. Mckee, D. W. Carbon 1988, 26, 659–665.
13. Mckee, D. W. Carbon 1985, 24, 737–741.
14. Clauss, F. J. Solid Lubricants and Self-lubricating Solids; Academic: New York, 1972; pp 43–74.